Experimental investigations on glass fibre reinforced composites with gypsum-earth matrix to strengthen the earth walls of the Noh-Gonbad Mosque in Balkh, Afghanistan

Arash Boostani, Giulia Misseri, Luisa Rovero* and Ugo Tonietti

Department of Architecture,
University of Florence,
Florence 50121, Italy
Email: arash.boostani@unifi.it
Email: giulia.misseri@unifi.it
Email: luisa.rovero@unifi.it
Email: ugo.tonietti@unifi.it
*Corresponding author

Abstract: The Noh Gonbad Mosque is an almost unknown masterpiece dated back to the 8th century, located near Balkh, North Afghanistan. The archaeological remains show different buildings techniques such as rammed earth (for portions perimeter walls), adobe masonry (for walls, niches and abutment of the arcades) and brick masonry with earth or gypsum mortar (for domes, arch and columns). The state of ruin required targeted intervention strategies for perimeter walls. The presence of collapse debris, and the possibility of their removal, would though increase, for the masonry portions, the vulnerability against overturning connected to the seismic hazard at the site. The reported experimental campaign focus on the identification of a fibre reinforced composite system aimed at jacketing perimeter walls. Tests address different matrix compositions compatible with the substrate, i.e., based on earth and gypsum. Results enable to highlight the effect that the composition has on the mechanical response.

Keywords: earth material; gypsum; glass fibre reinforced composites; mechanical tests; abbassid period mosque; Balkh, Afghanistan.

Biographical notes: Arash Boostani received his PhD in Structures and Restoration of Architecture and the Cultural Heritage from the University of Florence in 2019. He is currently managing conservation projects in Afghanistan. His research interests include traditional construction technology and structural restoration of historic buildings.

Giulia Misseri received her PhD in Structures and Restoration of Architecture and the Cultural Heritage from the University of Florence in 2017. She is currently an Assistant Professor of Structural Mechanics at the University of Florence. Her research interests include statics and dynamics of masonry structures, fracture mechanics and experimental testing.

Luisa Rovero is an Associate Professor of Structural Mechanics at Department of Architecture, University of Florence. She is a member of the Committee of the PhD Curriculum Structures and Restoration of Architecture and the Cultural Heritage of PhD Program in Architecture of the University of Florence. Her current research activity is mainly focused on mechanical behaviour of masonry structures, analysis and modelling of fibre-reinforced inorganic matrix materials for the reinforcement of masonry structures.

Ugo Tonietti is a Professor of Static and Stability of Masonry Structures at the Department of Architecture of the University of Florence. His research activity is focused on the mechanical behaviour of Masonry and Earthen Structures and on the consolidation strategies for historical buildings (based on compatibility and recovering of traditional building cultures). As an architect specialised in the conservation of cultural heritage, he studied and designed structural rehabilitations for historical and vernacular settlements and for world heritage sites.

1   Introduction

In the last decade, fibre reinforced cementitious matrix composites (FRCM), also known as textile reinforced mortars (TRM), were proposed for the reinforcement of masonry buildings in the form of strips to be applied on the surfaces. In fact, as regards the application to masonry structures, the FRCM reinforcement systems are much more suitable than the previously used FRP systems: FRCMs provide compatibility with the masonry substrate, reversibility, resistance to high temperatures and breathability (Alecci et al., 2016; Carozzi et al., 2016; Kouris and Triantafillou, 2018; Misseri et al., 2019a; Zampieri, 2020; Zampieri et al., 2018). Moreover, in FRP systems the transfer of the shear stress from the masonry structure to the composite takes place at the masonry-FRP strip interface, producing damage in the underlying masonry by delamination when failure occurs. Differently, in FRCM systems the actual stress transfer zone takes place at the matrix-fibre interface, where the common failures are debonding at the fibre-matrix interface and fibre slippage within matrix layers, (Barducci et al., 2020; De Santis et al., 2017; Misseri et al., 2019a; Ombres et al., 2018; Rotunno et al., 2014), without masonry substrate damage.

Different textile materials are used to implement the FRCM composite systems: glass, carbon, steel, PBO, basalt, and natural fibres (Barducci et al., 2020; Caggegi et al., 2017; Monaldo et al., 2019; Olivito et al., 2014) and different textile layouts are implemented, varying, for example, the size of the mesh, the type of knot between the weft and the warp and the treatment of the fibres, (Misseri et al., 2019b).

The greater suitability of FRCMs in the application on masonry is linked to the chemical physical nature of the matrices, which are inorganic mortars. The most common matrices are made up of cement or hydraulic lime mortar, both often improved with additives. Recently, Misseri et al. (2021a) and Rovero et al. (2020a), an innovative composite, made by a glass fibre textile embedded in a gypsum matrix, is proposed for

the reinforcement of architectural heritage structures in which the use of gypsum-based mortars for bedding joints, plasters and decoration is common, as is the case of many Mediterranean and Middle East countries (Azil et al., 2020; Boostani et al., 2018; La Spina et al., 2014; Vegas et al., 2012). Composites consisting of low-cost net, such as those made from plastic, metal, or natural fibres, embedded in earthen mortar, have been also proposed with the aim of finding solutions to mitigate the seismic vulnerability of earthen constructions, (Blondet et al., 2006, 2003; Blondet and Aguilar, 2007; Bove et al., 2016; Torrealva et al., 2008). The earth based architectural heritage includes poor settlements, in which more than a third of the world population live, buildings of the monumental heritage, and contemporary architectures that exploit the sustainable characteristics of the earth material, due to its low embodied energy, (Boostani et al., 2018; Egenti and Khatib, 2016; Fabbri et al., 2018; Fratini et al., 2011; Gamrani et al., 2012; Houben and Guillaud, 1994; Minke, 2000; Misseri et al., 2020; Rovero and Tonietti, 2012). Unfortunately, in addition to the many advantages, earthen material exhibits undesirable drawbacks due to poor mechanical characteristics and vulnerability to erosion due to weather conditions and rising damp.

In Blondet et al. (2006), strips of polymer net embedded in earthen mortar have been proposed to reinforce earthen constructions exposed to high seismic hazards. In particular, full-scale one-storey simple house models made of adobe masonry and with different types of polymer net were analysed by shaking table tests. Similar were carried out to evaluate the effectiveness of a nylon-rope net embedded in earthen mortar to reinforce earthen buildings, (Blondet et al., 2014; Lundgren et al., 2012). Retrofitting based on two types of natural fibres net (jute and a coconut) in earthen mortar have been investigated in Bove et al. (2016) through an experimental campaign and numerical analyses. In particular, the results of three-point bending tests on adobe bricks reinforced on the intrados with natural fibre composite strips were used to calibrate a non-linear numerical model.

In this paper, the case of the consolidation of the Noh Gunbad Mosque in Afghanistan, dated back to 790–800 A.D., (Boostani et al., 2020), is considered. The fragile perimeter walls, made of rammed earth blocks and adobe bricks, are investigated; the conservation state appears extremely poor. The walls showed a strong vulnerability with respect to buckling and horizontal out-of-plane actions, and the estimated seismic hazard of the region is remarkable.

Hence, a dedicated, earth-compatible, fibre-reinforced strengthening technique is investigated to provide adequate jacketing to the perimeter walls. The fibre reinforced composite is conceived balancing the need for a strong retrofitting action with the requirements of conservation interventions. Hence, the inorganic mortar matrix should be based on earth and gypsum. As for the reinforcing net, glass fibre is chosen since it shows lower strength and stiffness compared to other available options (e.g., carbon, kevlar, polybenzobisoxazole, basalt), this fact eases, on one hand, an efficient exploitation of the actual fibre capacity, and on the other, a closer behaviour, compared to other fibres, with the substrate.

To define adequate mechanical and workability characteristics of the mortar matrix, three-point bending, and compression tests encompassed a set of eight types of mortars showing variations in the earth-gypsum-water proportions. On a reduced set of samples, three-point bending tests on the composite lamina and on reinforced earth blocks are reported. Test results enable to highlight the appropriateness of the slurries and can support, from the scientific point of view, the implementation phase.

Figure 1   (a) plan in evidence the different materials (b) south wall, looking from the east
(see online version for colours)

(a)   (b)
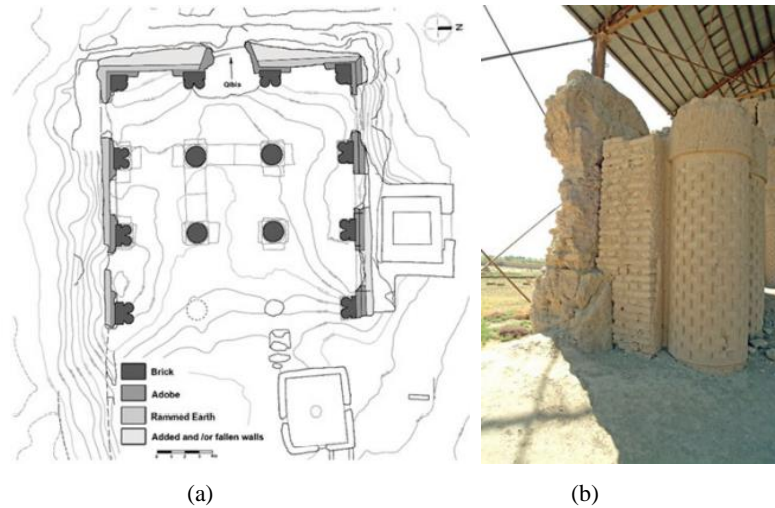
2   The Noh Gunbad Mosque and its perimeter walls

2.1   General overview

The Noh-Gonbad Mosque is located in the south-west of the ancient Balkh citadel, in the province of Mazar-el-Sharif. Until recently, (Adle, 2011; Chirvani, 1969; Golombek, 1969; Pougatchenkova, 1968), the ruins of Noh-Gonbad remained entirely unknown to the external world. As reported in Adle (2011), the Noh-Gonbad Mosque in Balkh is certainly the most ancient monumental mosque in Afghanistan, one of the oldest of the Islamic world, and has been object of a wide conservation campaign. The building has remarkable importance also due to its gypsum decorations, which appear today white or earthen colour, but used to be lapis-blue coloured, as archaeological surveys revealed. The monument's erection took place between 790–800 A.D., (Adle, 2011); and it was originally completed with nine domes, supported by fifteen arches resting on columns or semi-columns. The collapse of the domes only a few years after their completion, reasonably owed to a strong earthquake, left the monument in ruins and hidden, for the lower half of the columns, by a thick layer of debris.

The building is closed on three sides, 20 m each, by perimeter walls, Figure 1, all showing the signs of degradation processes. The system of arcades today visible consists in two deep rings, approximately 1.60 m including the decoration layer, and three columns. The arches' profiles are weakly pointed, with span around 5 m; ring thickness ranges 63–65 cm, Figure 2.

Figure 2 View of the Noh Gunbad Mosque (see online version for colours)

Figure 3 (a) West wall Mihrab (b) West wall (c) connection between the Mihrab and the west wall looking north (see online version for colours)

(a)

(b)

(c)

2.2   *Materials and building techniques*

Concerning perimeter walls, three layers placed side by side constitute the South and West portions. In these areas, different building technologies are recognisable: rammed earth constitutes the external and basement parts, the internal layer is an adobe masonry, and the inner part is made of baked bricks, coinciding with the columns that used to support the arches and domes, Figure 1(b). The North wall is, instead, almost entirely made in adobe masonry.

Figure 4   Internal view of South wall, central arch (see online version for colours)

The base structure of the South and West perimeter walls of the mosque, rests on a layer of rammed earth blocks, Figures 3(a) and 3(b). These blocks seem to have been cast in formwork, confirmed by the smooth surfaces at the edges of the blocks, Figure 3(b). This type of earthen masonry, about 90–100 cm thick, reaches approx. 2.5 m above ground level and was certainly built in a previous period, (Marquis et al., 2017), witnessing the presence of a previous building. The horizontal widths vary between 70–90 cm, with a consistent height of 90 cm. It is not clear if a single rammed earth block spans the whole thickness of the wall in all areas. In the South wall there is evidence that a single block of rammed earth is used, whereas in the West wall two 45–50 cm blocks are present Figure 3(c) laid side-by-side in the depth of the wall, possibly as a solution to implement the construction of the corner. For these walls, targeted excavations have highlighted the absence of any stone footing. Above the rammed earth base portion of the southern and western walls, around openings, a second layer of mud and brick was constructed to distribute the load of the large domes and as a ground layer for the application of decorations. The external rammed earth wall (thickness of 45 cm–50 cm, width varies between 70 cm–80 cm, height of 80 cm–90 cm) and the internal mud brick adobe wall

(average size of brick 32 × 32 × 6/7 cm), Figure 3(c), are sometimes woven together but more often act as independent walls. As a result, large cracks have developed. This internal brickwork skin was built with the specific aim of allowing for the more accurate form required for inner arches and niches. Where the thickness of the wall is reduced, as in the case of the niches in each span, the masonry is constituted by a thinner layer of rammed earth, with the exception of the highest parts of such niches in the western wall Figure 4.

Figure 5 Internal view of north wall (see online version for colours)

The western and northern walls exhibit a further layer of masonry on the outside. These sections are a mixed technique of earth roughly rammed and horizontal layers of bricks at the top, which may belong to more recent interventions. Moreover, at the base of the north wall, adobe masonry was employed. Evidence of this can be seen in the construction of the two arches enclosed in the north wall Figure 5 and in the brickwork visible in the north-eastern corner of the building.

2.3 *Conservation state and consolidation strategies*

What remains of the original structure suffered for many centuries from exposure to weathering and lacks an integrated and interconnected resistant system in which arches, columns and walls cooperate mechanically. Furthermore, exposure to seismic actions, rather frequent and intense in the area, constitutes an added source of vulnerability. The visible consequences of these actions are degradation of materials, severe crack patterns leading to equilibrium condition of the standing masonries close to the stability limit. The perimeter walls have clearly defined crack patterns consistent with fractures caused by motions resulting from the collapse of the domes. Concerning the vulnerability of perimeter walls, many parts of the system lost their consistency. Also, on the back of the twinned semi-columns, the wall is separated in two different layers due to the disconnection between the rammed earth and adobe masonry. Finally, both the niches of the South side of the wall exhibit great vertical cracks and loss of consistency and cohesion.

In synthesis, two are the main weaknesses affecting perimeter walls. The first is a consequence of the different construction techniques involved in the building; this situation has led, over time, to the almost complete separation of the parts built in different ways, i.e., led to the disconnection between rammed earth and adobe layers and between adobe layers and backed brick masonry, Figure 1(b). Such separation increases

the risk to overturning, since the wall, divided into three different layers exhibits three different rotation axes. A re-stitching of these different layers is hence necessary. Dedicated investigations to implement compatible and effective solutions for wall stitching are reported in Boostani et al. (2020).

Figure 6   Conservation state of the wall constituting a niche (see online version for colours)


A second weakness concerns the consistency of the parts that used to be buried by debris, especially the niches of the South wall, Figure 6. The consolidation of perimeter walls is necessary not only as a strengthening action able to preserve the masonry from damage and decay, but such intervention shall be carried out to improve safety margins against buckling and overturing, considering that the removal of the debris layer induces a consequent increase of the free height. Indeed, the presence of the debris has constituted a constraint for many centuries, reducing the height of the perimeter walls and their vulnerability to tilting. Therefore, to enable conservation and restoration of the monument, which requires the removal of the debris layer, adequate actions to improve structural safety margins must be pursued.

The need for serious improvement of such weaknesses requires the development of targeted consolidation strategies. They must address the specific vulnerabilities and define a mechanical retrofitting system compatible with the original materials and complying with the fundamental conservation issues. Only in this way, it is possible to find a balance between safety and safeguard. In this framework, earth-compatible, fibre reinforced strengthening technique is considered a viable and reasonable consolidation strategy to provide satisfactory jacketing of the niches of perimeter walls. Jacketing of earth walls makes it possible to counteract buckling and horizontal out-of-plane actions to which the perimeter walls can be subjected if hit by seismic actions. Other solutions, such as grout injections and buttressing were implemented

where possible. In those areas where the consistency of the walls and the decorative apparatus were irremediably lost (i.e., through thickness voids), jacketing was considered indispensable. Also, the layer of the earth-gypsum mortar matrix was accurately designed to join the original decorative band, and so as not to interfere the overall perception of the monument.

Figure 7 Three-point bending test on pure gypsum mortar (a) images from tests and (b) load displacement diagrams for type A4 (left) and A5 (right) (see online version for colours)

(a)

(b)
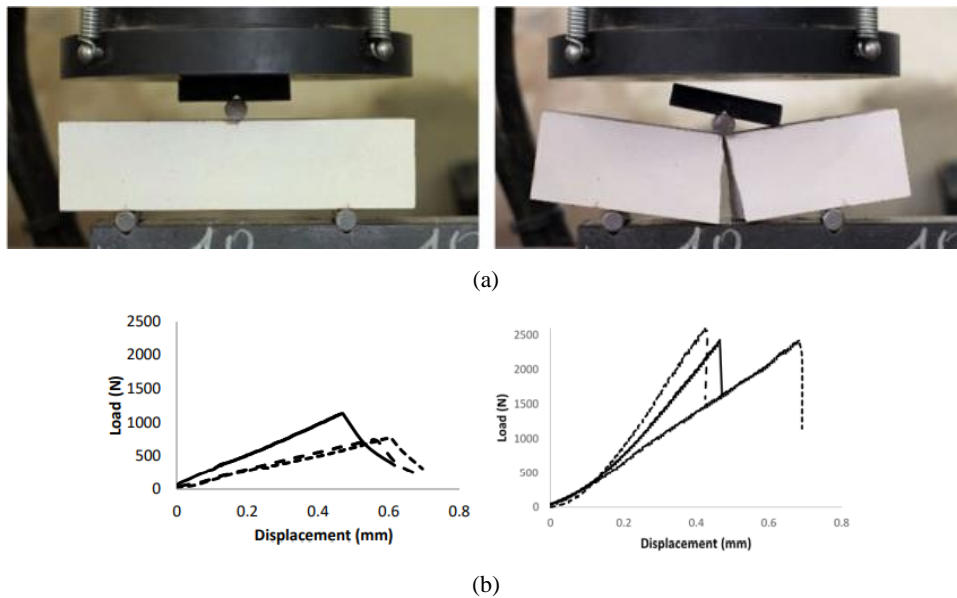
3 Experimental campaigns

3.1 Tests and specimens

An extensive campaign was carried out to choose a fibre-reinforced composite that could combine compatibility with the earthen substrate and efficiency in improving mechanical behaviour.

For the textile, the choice fell on a glass-fibre textile because it adapts better to an earth wall, since it is more deformable if compared to e.g., carbon-fibre ones, (Misseri et al., 2021b; Rovero et al., 2020b). A marketed product, (FibreNet, 2021), that uses thermo-welding technology on a dry mesh (i.e., no coating), is selected. The balanced bidirectional glass-fibre mesh has a mesh opening of 12 mm and an equivalent thickness of 0.0377 mm in both weft and yarn directions. Made of alkali-resistant (AR) glass fibres with zirconium oxide content greater than 16%, it is characterised by tensile strength of 1,400 MPa, elastic modulus 74 GPa, and minimum elongation at break equal to 2.0%, according to datasheet.

For the mortar matrix to couple with the glass fibre, the following tests, were carried out on 8 samples varying the gypsum-earth balance. All the test results are reported in Figures 7–20; in particular, the following tests were carried out

- Three-point bending and compression tests on 40 × 40 × 160 mm mortar prisms to characterise the intrinsic mechanical parameters of the matrixes (eight samples, three specimens each), see Figures 7(a) and 11(a).

- Three-point bending tests on 200 × 200 × 15 mm composite lamina to interpret the basic characteristics of the textile-matrix coupling (five samples, three specimens each), see Figure 15(a).

- Adhesion tests on blocks reinforced with 200 × 200 × 1 mm composite jacket to identify rammed earth block-composite interaction (five samples, three specimens each), see Figure 18.

Figure 8   Three-point bending test on mortar types B (left) and c (right) the mortars have the same gypsum-earth mix, sample B contains 0.2 part of resin (relative to weight)
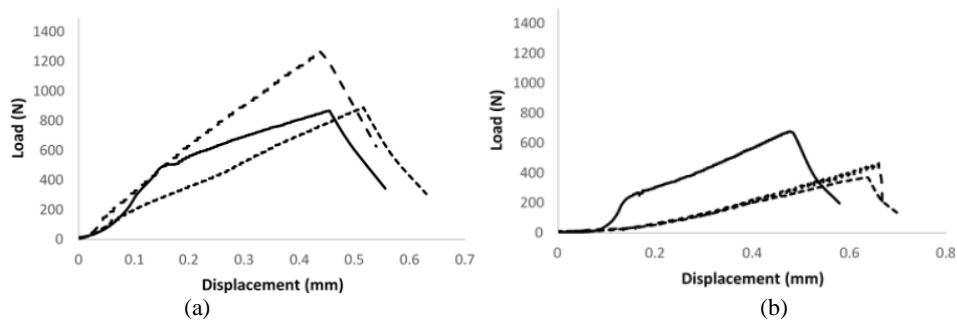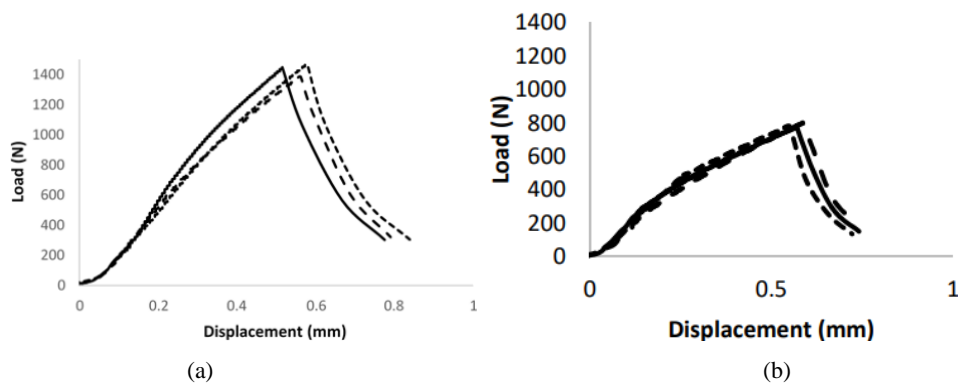

(a)   (b)

Figure 9   Three-point bending test on (a) mortar types D (left) and (b) E (right), the mortars have the same gypsum-earth mix, sample D contains 0.1 part of resin (relative to weight)

(a)   (b)

For all the tests, the aim is a comparative analysis between the performance of the mortar mixes, standalone or coupled with the glass fibre mesh, and the performance of the standalone block with respect to the reinforced one. Indeed, to the best of the authors'

knowledge, no similar system is available in the literature, and this campaign constitutes a first insight on the issue. Also, due to the fragility of the mortar and the related problems for the gripping of the specimen, standard characterisation protocols for FRCM systems are not straightforward to apply in this case. For these reasons, beam-tests rather than tensile tests on composite lamina and bond tests on a substrate have been considered here. However, further investigation is deemed necessary and currently going on.

Figure 10 Three-point bending test on (a) mortar types F (left) and (b) P (right), the mortars show the same gypsum-earth mix, sample P contains 0.005 part of short polypropylene fibres (relative to weight)

(a)   (b)
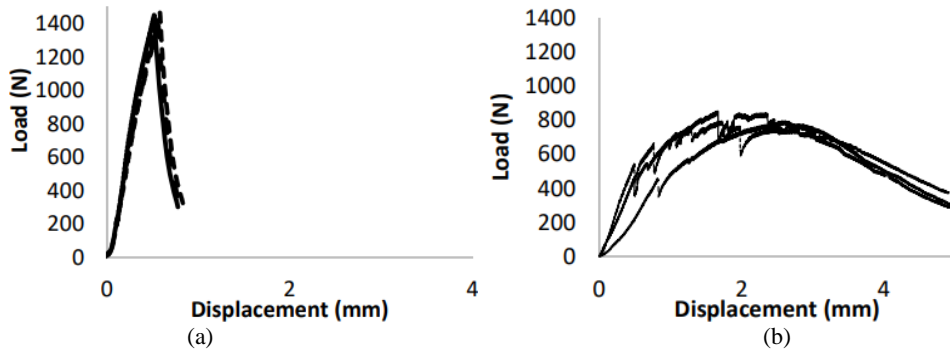
3.2 Characterisation of the matrix

A set of eight mixed earth-gypsum matrix samples (A4, A5, B, C, D, E, F, P) varying proportions were tested to identify an optimum balance. In two samples, resin and Polypropylene Fibres were added to the slurry, Table 1. The specimens were made using galvanised metal formwork. For each type of matrix, three specimens with dimensions of $40 \times 40 \times 160$ mm were tested. After 4 days, the specimens were removed from the mould and left to dry for 3 weeks.

Table 1 Mortar composition: mix ratio by weight

ID	Gypsum	Earth	Resin	PPF	Water
A4°	10				5
A5*	10				
B	6	4	2		
C	6	4			
D	4	6	41		
E	4	6			
F	2	8			
P	2	8	0.05		

Note: PPF = polypropylene fibres, roccastrada gypsum, *Afghan gypsum.

The raw earth employed for the matrices was collected on a selected site. The raw material was air-dried in a controlled environment. Then, sifting was carried out employing sieves in order to separate the following fractions: sand ($\phi > 63$ μm), silt

(4 μm ≤ φ ≤ 63 μm) and clay (φ < 4 μm). Results show a silty sand for the composition (54% of sand, 27.5% of silt and 18.5% clay).

Figure 11   Compression test on pure gypsum mortar (a) images from tests and (b) stress strain diagrams for types (left) A4 and (right) A5 (see online version for colours)
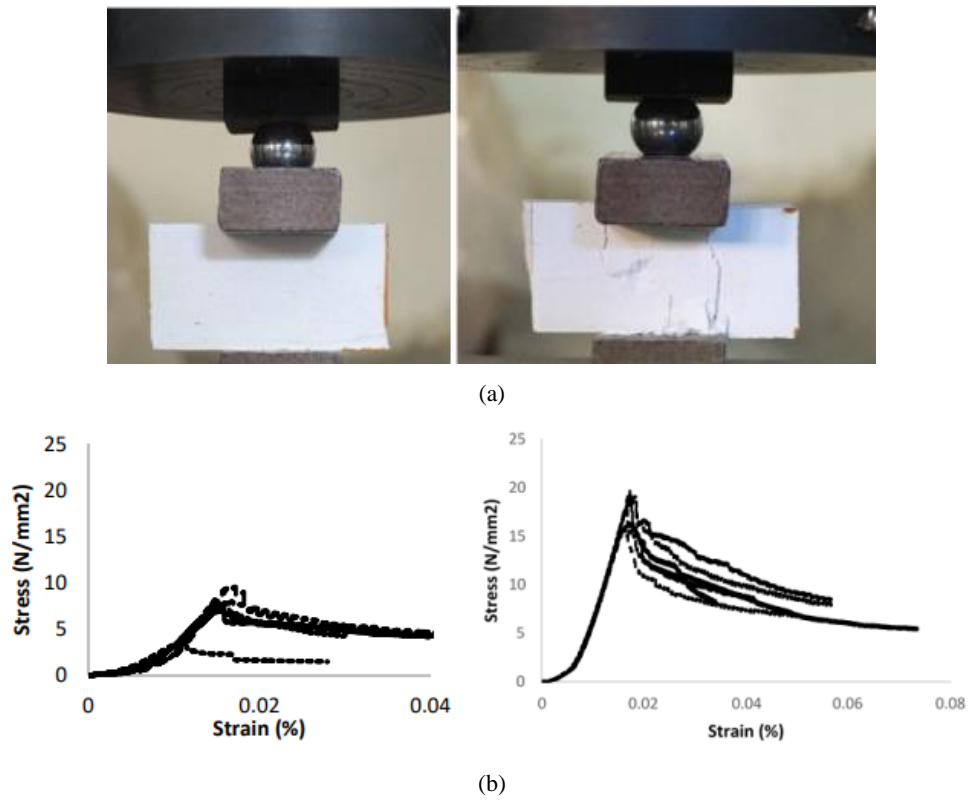

(a)

(b)

Figure 12   Compression test on (a) mortar B (left) and (b) C (right), the mortars have the same gypsum   earth mix, sample b contains 0.2 part of resin (relative to weight)

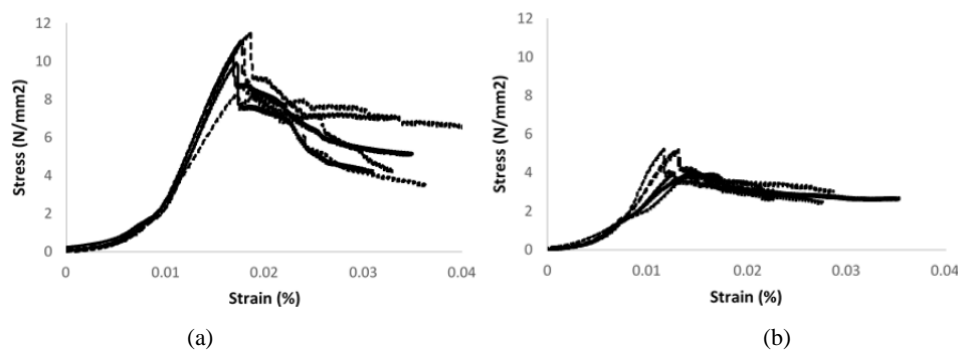(a)   (b)

Figure 13   Compression test on (a) mortar D (left) and (b) E (right), the mortars have the same gypsum Earth mix, sample d contains 0.1 part of resin (relative to weight)
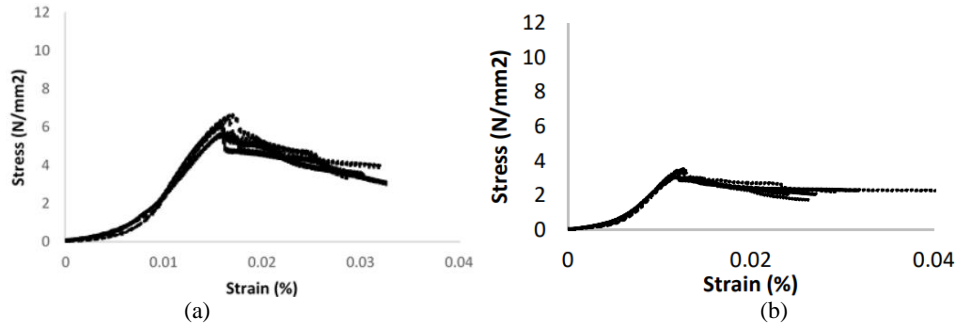

(a)

(b)

Figure 14   Compression test on (a) mortar types F (left) and (b) P (right); the mortars have the same gypsum-earth mix, sample P contains 0.005 part of short polypropylene fibres (relative to weight)
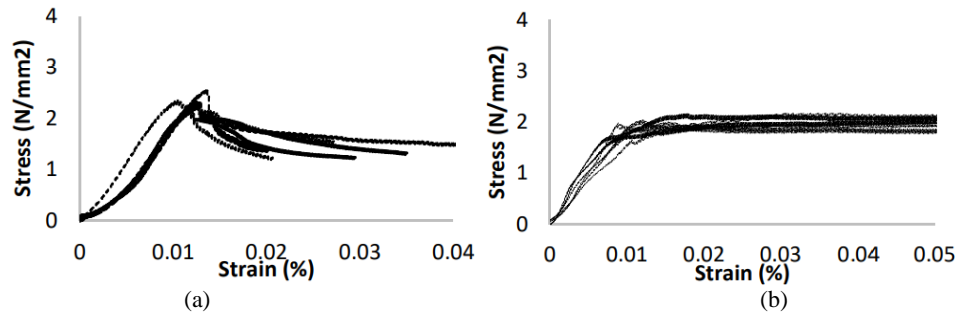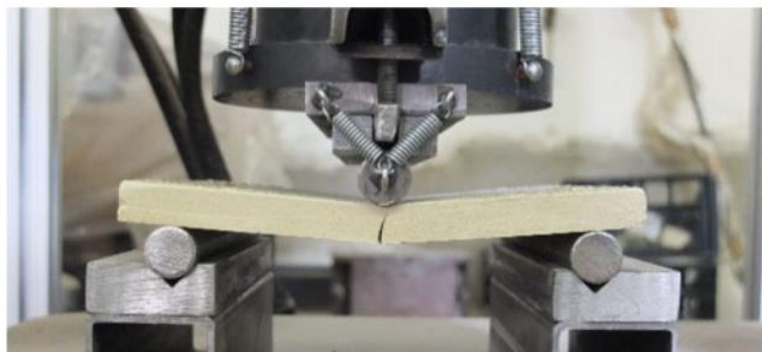

(a)

(b)

Figure 15   Three-point bending test on composite sheet (a) image from tests and (b) load displacement diagrams for matrix mortar types (left) A4 and (right) D (see online version for colours)

(a)

Figure 15   Three-point bending test on composite sheet (a) image from tests and (b) load
              displacement diagrams for matrix mortar types (left) A4 and (right) D (continued)
              (see online version for colours)

(b)   (c)
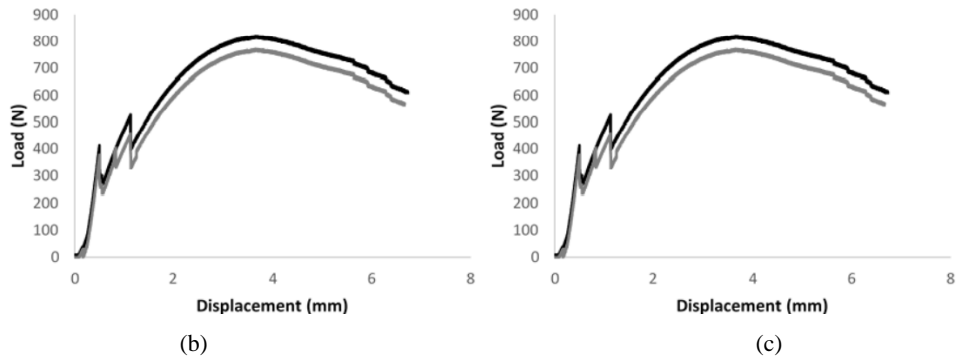
Figure 16   Three-point bending test on composite sheet with (a) matrix mortar types (left) E and
              (b) (right) E1; mortars have the same composition, but in E1 sample, mesh precoating
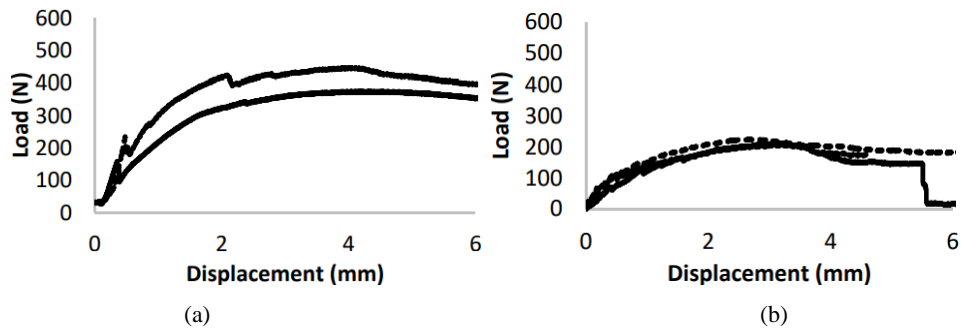   is applied

(a)   (b)
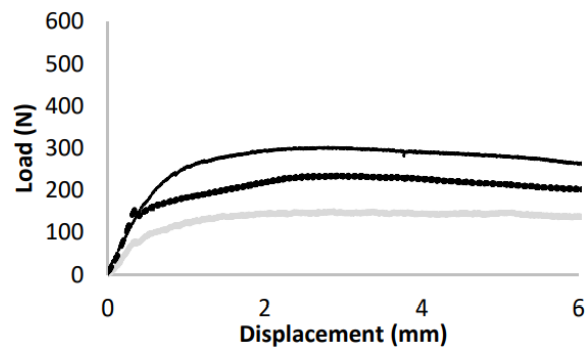
Figure 17   Three-point bending test on composite sheet with matrix mortar types P

Table 2   Results of three-point bending tests on mortar matrixes

ID	A4	A5	B	C	D	E	F	P
F_{max} [N]	876	2,486	1,016	502	1,434	783	569	816
C.o.V.	0.25	0.04	0.21	0.31	0.03	0.02	0.03	0.04
Δl_{max} [mm]	0.54	0.53	0.47	0.59	0.55	0.57	0.80	1.99
C.o.V.	0.12	0.25	0.09	0.17	0.06	0.04	0.01	0.27
σ [MPa]	2.05	5.88	2.37	1.18	3.36	1.84	1.45	1.98
C.o.V.	0.25	0.03	0.22	0.31	0.03	0.02	0.02	0.04

Table 3   Results of compression tests

ID	A4	A5	B	C	D	E	F	P
F_{max} [kN]	12.32	28.83	16.62	7.43	9.85	5.46	3.73	3.48
C.o.V.	0.28	0.09	0.11	0.13	0.06	0.05	0.05	0.13
Δl [mm]	0.62	0.68	0.7	0.53	0.65	0.50	0.49	3.22
C.o.V.	0.16	0.04	0.04	0.08	0.03	0.03	0.08	1.13
σ_{max} [Mpa]	8.49	18.02	10.39	4.64	6.16	3.42	2.33	2.21
C.o.V.	0.13	0.13	0.11	0.13	0.06	0.05	0.05	0.13
E_c [GPa]	1.07	1.68	*1.14*	0.69	*0.71*	0.47	0.26	0.22
C.o.V.	0.23	0.05	0.15	0.36	0.13	0.09	0.09	0.21
μc [–]	1.05	1.01	1.04	1.00	1.06	1.03	1.07	5.48
C.o.V.	0.07	0.02	0.02	0.12	0.03	0.03	0.04	0.91
μcd [–]	1.17	1.14	1.21	1.21	1.23	1.27	1.27	0.18
C.o.V.	0.12	0.05	0.31	0.17	0.12	0.15	0.13	2.26

Notes: F_{max}: peak load, Δl displacement at peak load, σ_{max}: compressive strength, E_c:
   compressive Young's modulus, μ_c: kinematic ductility, μ_{cd}: available kinematic
   ductility.

The gypsum matrix powder employed for sample A4 (GessiRoccastrada, 2021) consists of a mix of α and β hemi-hydrated calcium sulphate. The gypsum powder employed for A5 sample was supplied by an Afghan producer ('Gache-e Setâre'). For both the A4 and A5 samples, a 1:1 water-to-binder ratio was considered, differently from (Rovero et al., 2020b). The resin employed in two mortar mixes consists in a two-phase mix made from two resins supported on an inorganic matrix and microcrystalline thixotropic. In the polymerisation phase, the resin creates a lattice interpenetrated that reinforced by the microcrystals of the inorganic phase. The resin is resistant to alkaline environments, does not show thermal transitions of the second order, and does not burn. The microcrystalline, thixotropic matrix is characterised, according to the manufacturer data sheet, by a flexural strength of 5 MPa, a flexural elastic modulus of 50 MPa and by more than 1.2% ultimate tensile elongation at break.

   To determine the mechanical parameters of mortars, three-point bending tests and uniaxial compression tests were carried out according to EN1015-11 (CEN, 2019), but considering 0.5mm/min displacement rate to capture also the post-peak phase.

   Results of the three-point bending tests on mortar matrix prisms in terms of load deflection diagrams are reported in Figures 7, 8, 9 and 10. Relevant results, in terms of

maximum force (F_{max}) deflection at maximum force (Δl_{max}) and peak stress (σ), are summarised in Table 2. As for compression tests, the stress-strain diagrams are reported in Figures 11, 12, 13 and 14. The elastic modulus in compression (E_c) is evaluated at one third of the peak stress reached. Kinematic ductility ($\mu_c=xM/xL'$) and available kinematic ductility ($\mu_{cd}= xU/xM$) identifying the pre-peak and post-peak non-linear capacity of the mortar, respectively, are evaluated as in, e.g., (Azil et al., 2020), see Figure 21.

Test results enable the following considerations:

- Pure gypsum mortars, A4 and A5, show a remarkable capacity in bending (2.05 MPa and 5.88 MPa) and compression (8.49 MPa and 18.82 MPa). The Afghan gypsum (A5) showed remarkably higher force capacity and comparable deflections, the noticeable variability is connected to the firing temperature, the chemical composition of the raw gypsum stone employed.

- Samples with increasing amounts of earth (samples C, E and F, 40%, 60% and 80% respectively) show higher displacement capacity at peak load (in compression and bending), lower compressive strength and lower Young's modulus compared to pure Gypsum samples (A4 and A5, 100% gypsum). Hence, gypsum amount is directly proportional to compressive strength and Young's modulus; linear regression on results of the types A4, C, E, F, (i.e., with same gypsum and no added resin) provided a coefficient of determination $R^2 = 0.98$ and $R^2 = 0.99$, respectively. Also, while the kinematic ductility, μ_c, is substantially insensitive to gypsum amount, the available kinematic ductility, μ_{cd}, decreases linearly ($R^2 = 0.91$) with the increase in gypsum amount.

- Results of compressive tests on sample F (80% earth) are in line with other investigations, e.g., (Clementi et al., 2008; Lenci et al., 2012, 2011).

- Adding microcrystalline resin to the gypsum-earth mix induces remarkable stiffness increase and ductility decrement. Comparing samples B, D with samples C and E (no resin, same gypsum-earth ratio), respectively, it can be seen a +65% (sample B) and +51% (sample D) in the elasticity modulus. For compressive strength, +123% (sample B) and +80% (sample D) is recorded.

- The highest Yong's modulus, apart from sample A5, is recorded for the sample with the highest amount of resin, i.e., B, 6.4% greater than the pure gypsum mortar sample A4 modulus ($E_c = 1.07$ GPa).

- Adding propylene fibres to the F type mix, obtaining P sample, does not affect the stiffness or the strength in compression, and greatly improves the pre-peak displacement capacity in bending, where the failure mode passe from brittle after a linear ascending branch, to non-linear pre-peak evolution and quadratic softening branch.

3.3   *Characterisation of the composite laminas*

A subset of samples, i.e., A4, D, E and P, was selected to produce glass-fibre   reinforced composite laminas. A further sample that shows the same matrix composition of sample E, but differs in specimen preparation, detailed in the following, is labelled E1. Specimens were labelled according to the type (i.e., composite sheet, Cs) and alphabetic codes to refer to mortar type employed, see previous section.

The 200 × 200 × 15 mm specimens were built applying the first layer of the matrix mortar in the mould. The glass fibre net sheet was put on top of the fresh mortar, for the E1 sample a thin layer polycrystalline resin is applied on both sides of the net before placing it on the fresh matrix. Then the upper layer of the matrix mortar matrix was laid on. After three days the mould was removed, and the specimen was left for three weeks to dry at environmental temperature.

Each specimen was placed on two steel cylindrical supporting pins with 15 mm diameters located at a distance of 80 mm from the midline of the specimen. The vertical load was applied to the centre line using an additional steel cylinder with a 15 mm diameter interposed between the specimen and the load cell. The three-point bending tests were conducted under displacement control at a speed of 0.5 mm/min. The acquisition of the displacement measures took place through a linear variable differential transformer (LVDT) integrated into the test machine.

Figure 18   Load deflection diagrams (left) and images (right) from three-point bending test on (a) unreinforced rammed earth blocks and (b) on reinforced blocks with matrix type d

(a)

(b)
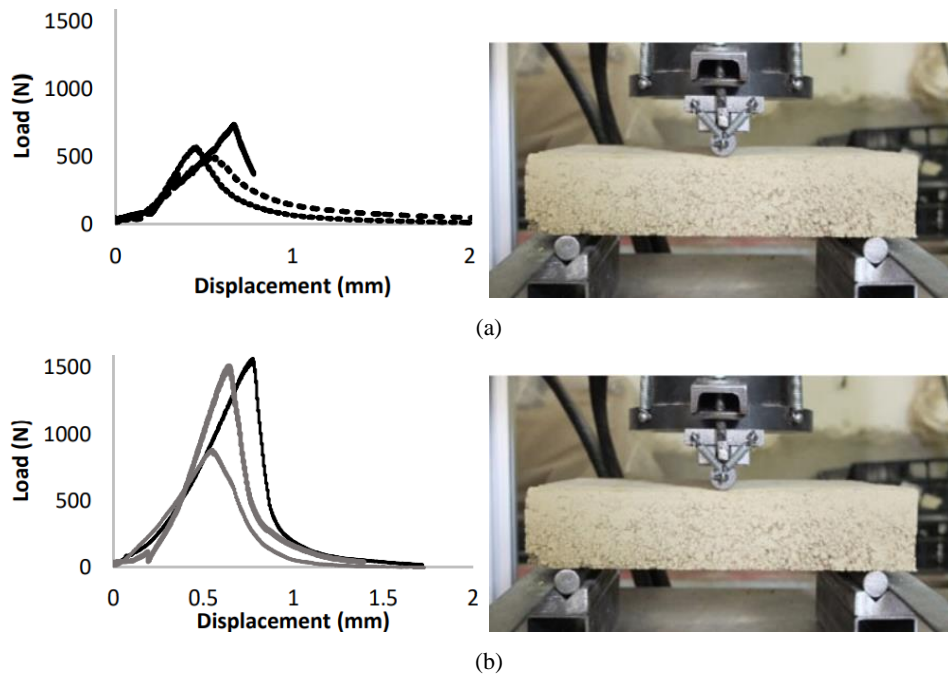
Results, reported in terms of load – deflection diagrams, are illustrated in Figures 15, 16 and 17. The tested specimens showed a similar failure mode. After a first initial linear elastic phase, cracking of matrix occurred at midspan extrados. Depending on the matrix brittleness, the mortar cracking was detectable on the diagrams, with load jumps, or with smoother loss of stiffness highlighted by a non-linear elastic branch, Figures 15–17. As a general trend, also for this set of tests, the decrease in gypsum amount provided a decrease in the bearing capacity. Moreover, for the composite lamina type A4, the mortar cracking load is nearly half the peak load reached. For Cs-D, the failure mode is similar, although only one specimen shows a load increase with higher peak in the post-cracking phase. For Cs-E the cracking phase is less pronounced, and the

peak load is reached through a smoothly increasing curve. The mesh pre-coating applied in the E1 sample, which has the same E matrix, is detrimental for bonding. This phenomenon is markedly different from what it is generally observed in standard FRCM systems, where resins coating is targeted at improving matrix-fibre or matrix-substrate adhesion. This fact is reasonably connected to the grain size of the mixed earthen-gypsum matrix which are sensibly littler than the standard sand grains found in lime and cement mortars. This fact enables deep imbuement of fibres, and hence good bonding. When instead the fibre interface is smoothed, the low mechanical capacity of the mortar plays its role.

The tests showed good adhesion between the net and the matrix in all samples except sample Cs-E1. In this sample, the net was located between two layers of microcrystalline resin, and the connection between the gypsum mortar was interrupted by a thin layer of resin. The connection between the resin and the upper matrix mortar was not strong. Sample P shows a higher displacement capacity and a remarkably low load level, while the specimens with higher amount of gypsum are stiffer, more resistant and show a brittle crack-driven failure.

Figure 19   Three-point bending test on reinforced blocks with (a) matrix mortar types E (left) and (b) E1 (right) mortars have the same composition, but in E1 sample, mesh precoating is applied
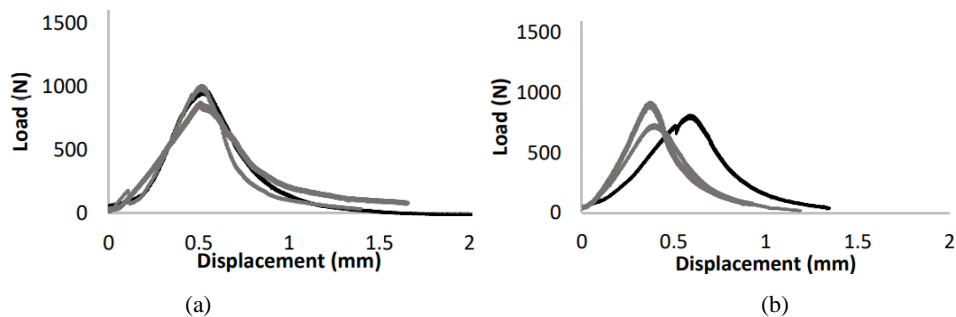

(a)   (b)

Figure 20   Three-point bending test on reinforced blocks with matrix mortar types P
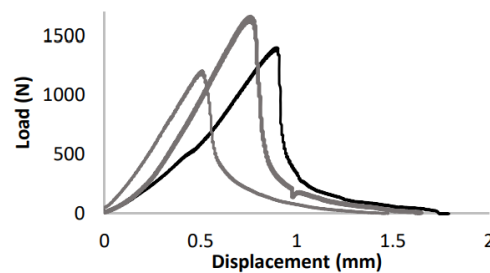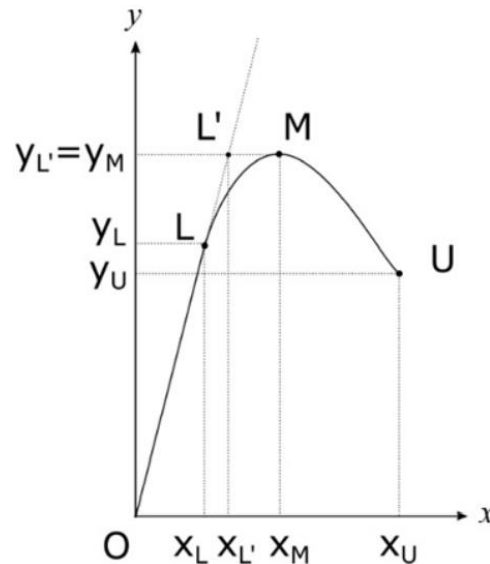
Figure 21   Relevant points of the reference load displacement diagram of uniaxial compression tests to evaluate mechanical parameters

3.4 Characterisation of reinforced blocks

Twenty-one rammed earth blocks of dimension $300 \times 220 \times 60$ mm were produced. The earth was dried using an electric ventilated oven for 24 hours at 60°C. Then, the dried earth was sieved using a 2 mm-mesh. After weight measurement of the earth, 11% water was added to the dry weight of the earth and the mixture was mixed for 5 minutes using an electric mixer on low speed to obtain a homogeneous wet earth to make rammed earth blocks. Three earth blocks were tested without fibre reinforced composite lamina. A three-point bending test was carried out, and 2 blocks $60 \times 60 \times 60$ mm obtained for each bending test were employed for the compression test. Nineteen rammed earth blocks were reinforced with a composite lamina $200 \times 200 \times 15$ thickness applied on the intrados surface of the blocks. The fibre reinforced composite sheets were made with the same glass fibre net and with the gypsum-earthen based mortar matrices D, E, E1 and P. In order to apply the composite sheet, a 15mm height wooden frame with the internal size of 200×200 mm was fixed on the upper surface of the rammed earth block. After spraying a bit of water on the surface of the block to avoid immediate water absorption by the rammed earth, the first layer of the matrix mortar was applied on the surface of the block inside the wooden mould. The pieces of 200×200 mm glass fiber net were applied on top of the fresh mortar and then the last part of the matrix mortar was applied on the top. The extra mortar was cleaned with a flat piece of metal to reach a smooth and flat surface. After three days the mould was removed, and the specimen was left to dry for three weeks. Specimens were labelled according to the test carried out, reinforced block (RB), and matrix composition.

Each specimen was placed on two steel cylindrical supporting pins with 15 mm diameters located at a distance of 125 mm from the specimen's median line. The vertical load was applied to the centre line using an additional steel cylinder with a 15 mm

diameter interposed between the specimen and the load cell. The tests were conducted under displacement control at a speed of 0.5 mm/min.

Results of adhesion tests show that the peak load is greatly increased by the presence of the composite sheet. The highest force and displacement capacity increment was provided by composite lamina type P, up to more than double when compared to the unreinforced block, see Figure 18(a) and Figure 20. Composite type P provided also greater deflections to the reinforced block when compared to the types E and E1, +39% and +60%, respectively.

The same quality of the load displacement diagrams, which are characterised by a linear elastic branch up to peak load followed by a non-linear descending failure, can be seen in Figures 18, 19 and 20. Indeed, owing to the good bond quality between the fibre and the matrixes, and the rammed earth block dimensions, which are rather stocky for manageability reasons, end-delamination of the reinforcing lamina was recorded, see Figure 18(b). Future investigations might consider more slender proportions for the substrate block to ease bending and four-point bending layout of the test to reduce shear stress effects.

Comparing results of types D, E, E1 and P, and bearing in mind the end delamination failure mode, it can be stated that the difference in force capacity, provides an estimation of the adhesive capacity of the reinforcing lamina to the block. Matrix type P, the richest in earth content provided the best adhesion properties, the peak load reached was remarkably greater than the values obtained for matrix types E and E1 (+49% and +73% respectively), Figure 18. This fact might be connected probably to the chemical bonding between clay grains of the block and the mortar. However, the activation of chemical bonding shall be heterogeneously distributed since remarkable data dispersion is recorded.

Also, the higher percentage of gypsum in the slurry (types D, E and E1) compared to type P does not ease adhesive capacity, unless resin additives are provided (E, E1). Despite this, the inclusion of resin in the gypsum-rich slurry (type E), provided the best clustering of results with values of coefficient of variation between 50%–90% lower than composite types D and P without resin.

Table 4   Results of three-point bending tests on composite lamina; F_{max}: peak load, Δl displacement at peak load

ID	A4	D	E	E1	P
Fmax [N]	796	330	411.58	214	230
C.o.V.	0.04	0.46	0.12	0.05	0.33
Δl_{max} [mm]	3,645	2.90	4.15	3.01	2.88
C.o.V.	0.00	0.57	0.06	0.07	0.03

Table 5   Results of three-point bending tests on reinforced blocks; F_{max}: peak load, Δl displacement at peak

	URB	D	E	E1	P
F_{max} [N]	604	1,322	953	820	1,423
C.o.V.	0.20	0.29	0.07	0.11	0.16
Δl_{max} [mm]	0.557	0.656	0.516	0.451	0.722
C.o.V.	0.19	0.18	0.02	0.27	0.27

4 Conclusions

The paper reports the outcomes of an experimental campaign dedicated to defining the most appropriate conservation technique for the perimeter walls of the Noh Gunbad mosque in Afghanistan. The different building techniques characterising the 12 centuries-old perimeter walls are based on raw earth blocks (rammed earth, adobe) and required a targeted jacketing intervention; a specifically designed fibre composite system was investigated with this aim. To the best of the authors' knowledge, no comparable system has ever been tested before, hence the novel results reported here can contribute to the development of further investigations. It is also worth noting that once the experimental campaign reported in the study ended, the actual intervention has been implemented on site. The implemented solution stood the test of three medium-low earthquake events.

The study focuses on the experimental campaign aimed at defining the most suitable gypsum-based matrixes to combine with a dry, alkali resistant glass fibre mesh. Results show that balancing earth-gypsum proportions in the mortar slurry enables it to reach an adequate flexural strength and displacement capacity. The two relatively weak binders, traditionally employed in the building technology culture of Central Asia, proved effective. Adapting such a solution to other contexts in the future, with adequate waterproofing treatments, appears reasonable, especially considering the low environmental footprint for their production.

Despite the established knowledge of earth and gypsum as binders in specific cultures, systematic investigation is lacking, and the reported test results can contribute to a sounder understating. For example, tests on the mixed earth-gypsum mortars show that adding short propylene fibres or microcrystalline resin significantly improves displacement capacity in bending and stiffness in compression. Also, resin applied as fibre-matrix adhesion booster turns out to be detrimental for bonding, reasonably due to the hindering effect to deep imbuement of glass fibres, possible for the small grain size of the mortar aggregates. Indeed, the three-point bending tests on composite lamina show a good bond behaviour and adhesion tests on rammed earth blocks resulted in end-delamination of the composite sheet for all tested cases.

In conclusion, it is also worth noting that the work carried out made it possible to deal with a case of structural reinforcement on a very complex architectural heritage building and was based on a selected experimental methodology suitable for the particular materials considered for the reinforcement. The experimental data obtained made it possible to optimise the mortar mixture to be used as matrix of the FRCM reinforcement system.

The case study analysed had very specific characteristics (pisè walls, use of gypsum as mortar binder, difficult environmental context) not allowing the use of standardised and already predefined solutions for the reinforcement system. The selection of materials on which to base the reinforcement solutions had therefore to be carefully evaluated, balancing safety requirements (evaluation of the mechanical properties of the components, adhesive capacity of the fibre-matrix and matrix-earth substrate) and safeguard requirements (material and mechanical compatibility, reversibility, minimal intervention).

References

Adle, C. (2011) 'La mosquée Hâji Piyâdah/Noh-Gonbadân à Balkh (Afghanistan)', *CRAI–Comptes Rendus Des Séances L'académie Des Inscriptions B-Lett.*, Vol. 1, pp.565–625.

Alecci, V., Misseri, G., Rovero, L., Stipo, G., De Stefano, M., Feo, L. and Luciano, R. (2016) 'Experimental investigation on masonry arches strengthened with PBO-FRCM composite', *Compos. Part B Eng.*, Vol. 100, pp.228–239, https://doi.org/10.1016/j.compositesb.2016.05.063.

Azil, C., Djebri, B., Fratini, F., Misseri, G. and Rovero, L. (2020) 'Desert rose stone constructions covered with domes in the Souf Region (Algeria)', *Int. J. Archit. Herit.*, Vol. 1, pp.1–20, DOI: 10.1080/15583058.2020.1813353.

Barducci, S., Alecci, V., De Stefano, M., Misseri, G., Rovero, L. and Stipo, G. (2020) 'Experimental and analytical investigations on bond behavior of Basalt FRCM systems', *J. Compos. Constr.*, Vol. 24, https://doi.org/10.1061/(ASCE)CC.1943-5614.0000985.

Blondet, M. and Aguilar, R. (2007) 'Seismic protection of earthen buildings', in *Conferencia Internacional En Ingenieria Sismica*.

Blondet, M., Torrealva, D., Vargas, J., Velasquez, J. and Tarque, N. (2006) 'Seismic reinforcement of adobe houses using external polymer mesh', in *First European Conference on Earthquake Engineering and Seismology*.

Blondet, M., Vargas, J., Sosa, C. and Soto, J. (2014) 'Using mud injection and an external rope mesh to reinforce historical earthen buildings located in seismic areas', in *Nineth International Conference on Structural Analysis of Historical Constructions*.

Blondet, M., Villa García, G. and Loaiza, C. (2003) 'Viviendas sismorresistentes de tierra?', in *Una Visión a Futuro, XIV Congreso Nacional de Ingeniería Civil*.

Boostani, A., Fratini, F., Misseri, G., Rovero, L. and Tonietti, U. (2018) 'A masterpiece of early Islamic architecture: the Noh-Gonbad Mosque in Balkh, Afghanistan', *J. Cult. Herit.*, Vol. 32, https://doi.org/10.1016/j.culher.2018.02.001.

Boostani, A., Misseri, G., Rovero, L. and Tonietti, U. (2020) 'The consolidation strategy of the Noh Gonbad Mosque vestiges in Balkh (Afghanistan)', *Procedia Struct. Integr.*, Vol. 29, pp.79–86, https://doi.org/10.1016/J.PROSTR.2020.11.142.

Bove, A., Misseri, G., Rovero, L. and Tonietti, U. (2016) 'Experimental and numerical analyses on the antiseismic effectiveness of fiber textile for earthen buildings', *J. Mater. Environ. Sci.*, Vol. 7, No. 10, pp.3548–3557.

Caggegi, C., Carozzi, F.G., De Santis, S., Fabbrocino, F., Focacci, F., Hojdys, Ł., Lanoye, E. and Zuccarino, L. (2017) 'Experimental analysis on tensile and bond properties of PBO and aramid fabric reinforced cementitious matrix for strengthening masonry structures', *Compos. Part B Eng.*, Vol. 127, pp.175–195, https://doi.org/10.1016/j.compositesb.2017.05.048.

Carozzi, F.G., Colombi, P., Fava, G. and Poggi, C. (2016) 'A cohesive interface crack model for the matrix-textile debonding in FRCM composites', *Compos. Struct.*, Vol. 143, pp.230–241, https://doi.org/10.1016/j.compstruct.2016.02.019.

CEN, (2019) *EN 1015-11 Methods of test for Mortar for Masonry – Part 11: Determination of Flexural and Compressive Strength of Hardened Mortar*.

Chirvani, A.S.M. (1969) 'La plus ancienne mosquée de Balkii', *Arts Asiat.*, Vol. 20, pp.3–20.

Clementi, F., Lenci, S. and Sadowski, T. (2008) 'Fracture characteristics of unfired earth', *Int. J. Fract.*, Vol. 149, pp.193–198.

De Santis, S., Ceroni, F., de Felice, G., Fagone, M., Ghiassi, B., Kwiecień, A., Lignola, G.P., Morganti, M., Santandrea, M., Valluzzi, M.R. and Viskovic, A. (2017) 'Round Robin test on tensile and bond behaviour of steel reinforced grout systems', *Compos. Part B Eng.*, Vol. 127, pp.100–120, https://doi.org/10.1016/j.compositesb.2017.03.052.

Egenti, C. and Khatib, J.M. (2016) 'Sustainability of compressed earth as a construction material', *Sustain. Constr. Mater.*, pp.309–341, https://doi.org/10.1016/B978-0-08-100370-1.00013-5.

Fabbri, A., Morel, J-C. and Gallipoli, D. (2018) 'Assessing the performance of earth building materials: a review of recent developments', *RILEM Tech. Lett.*, Vol. 3, pp.46–58, https://doi.org/10.21809/rilemtechlett.2018.71.

FibreNet, (2021) FB-VAR220R12 [online] https://www.fibrenet.it/product/fb-var220r12 (accessed 2 March 2022).

Fratini, F., Pecchioni, E., Rovero, L. and Tonietti, U. (2011) 'The earth in the architecture of the historical centre of Lamezia Terme (Italy): characterization for restoration', *Appl. Clay Sci.*, Vol. 53, pp.509–516, https://doi.org/10.1016/J.CLAY.2010.11.007.

Gamrani, N., R'kha Chaham, K., Ibnoussina, M., Fratini, F., Rovero, L., Tonietti, U., Mansori, M., Daoudi, L., Favotto, C. and Youbi, N. (2012) 'The particular 'rammed earth' of the Saadian sugar refinery of Chichaoua (XVIth century, Morocco): mineralogical, chemical and mechanical characteristics', *Environ. Earth Sci.*, Vol. 66, pp.129–140, https://doi.org/10.1007/S12665-011-1214-6/TABLES/8.

GessiRoccastrada (2021) TB40 [online] https://www.gessiroccastrada.com/it/tb-40.html (accessed 2 March 2022).

Golombek, L. (1969) 'Abbasid Mosque at Balkh', *Orient. Art*, Vol. 15, No. 3, pp.173–189.

Houben, H. and Guillaud, H. (1994) *Earth Construction: A Comprehensive Guide*, ed., ITDG Publi., Londono.

Kouris, L.A.S. and Triantafillou, T.C. (2018) 'State-of-the-art on strengthening of masonry structures with textile reinforced mortar (TRM)', *Constr. Build. Mater.*, https://doi.org/10.1016/j.conbuildmat.2018.08.039.

La Spina, V., Fratini, F., Cantisani, E., Mileto, C. and López-Manzanares, F.V. (2014) 'The ancient gypsum mortars of the historical façades in the city center of Valencia (Spain)', *Period. di Mineral.*, Vol. 82, No. 3, pp.443–457.

Lenci, S., Clementi, F. and Sadowski, T. (2012) 'Experimental determination of the fracture properties of unfired dry earth', *Eng. Fract. Mech.*, Vol. 87, pp.62–72, https://doi.org/10.1016/J.ENGFRACMECH.2012.03.005.

Lenci, S., Piattoni, Q., Clementi, F. and Sadowski, T. (2011) 'An experimental study on damage evolution of unfired dry earth under compression', *Int. J. Fract.*, Vol. 2011, pp.193–200, https://doi.org/10.1007/S10704-011-9651-5.

Lundgren, K., Kettil, P., Hanjari, K.Z., Schlune, H. and Soto, A. (2012) 'Analytical model for the bond-slip behaviour of corroded ribbed reinforcement', *Struct. Infrastruct. Eng.*, Vol. 8, pp.157–169, https://doi.org/10.1080/15732470903446993.

Marquis, P., Bendezu-Sarmiento, J., Lorain, T. and Rassuli, N. (2017) 'Haji Piada/Noh Gonbad: works carried out by French Archaeological delegation', in Secco Suardo, L. (Ed.): *The Nine Domes of the Universe*, *The Ancient Noh Gunbad Mosque. The Study and Conservation of an Early Islamic Monument at Balkh*, pp.49–59, Bolis, Rome.

Minke, G. (2000) *Earth Construction Handbook : The Building Material Earth In Modern Architecture*, WIT Press, Southampton, UK.

Misseri, G., Palazzi, C. and Rovero, L. (2020) 'Seismic vulnerability of timber reinforced earthen structures through standard and non–standard limit analysis', *Eng. Struct.*, Vol. 215, p.110663, https://doi.org/10.1016/j.engstruct.2020.110663.

Misseri, G., Rovero, L. and Galassi, S. (2021a) 'Analytical modelling bond behaviour of polybenzoxazole (PBO) and glass fibre reinforced cementitious matrix (FRCM) systems coupled with cement and gypsum matrixes: effect of the cohesive material law (CML) shape', *Compos. Part B Eng.*, Vol. 223, p.109090, https://doi.org/10.1016/J.COMPOSITESB.2021.109090.

Misseri, G., Rovero, L. and Galassi, S. (2021b) 'Analytical modelling bond behaviour of polybenzoxazole (PBO) and glass fibre reinforced cementitious matrix (FRCM) systems coupled with cement and gypsum matrixes: effect of the cohesive material law (CML) shape', *Compos. Part B Eng.*, Vol. 223, p.109090, https://doi.org/10.1016/J.COMPOSITESB.2021.109090.

Misseri, G., Rovero, L., Stipo, G., Barducci, S., Alecci, V. and De Stefano, M. (2019a) 'Experimental and analytical investigations on sustainable and innovative strengthening systems for masonry arches', *Compos. Struct.*, Vol. 210, https://doi.org/10.1016/j.compstruct.2018.11.054.

Misseri, G., Stipo, G., Galassi, S. and Rovero, L. (2019b) 'Experimental investigation on the bond behaviour of basalt trm systems-influence of textile configuration and multi-layer application', *Key Engineering Materials*, https://doi.org/10.4028/www.scientific.net/KEM.817.134.

Monaldo, E., Nerilli, F. and Vairo, G. (2019) 'Basalt-based fiber-reinforced materials and structural applications in civil engineering', *Compos. Struct.*, Vol. 214, pp.246–263, https://doi.org/10.1016/J.COMPSTRUCT.2019.02.002.

Olivito, R.S., Cevallos, O.A. and Carrozzini, A. (2014) 'Development of durable cementitious composites using sisal and flax fabrics for reinforcement of masonry structures', *Mater. Des.*, Vol. 57, pp.258–268, https://doi.org/10.1016/J.MATDES.2013.11.023.

Ombres, L., Mancuso, R., Nicol, M.S. and Verre, S. (2018) 'Bond between carbon fabric-reinforced cementitious matrix and masonry substrate', *J. Mater. Civ. Eng.*, Vol. 31, p.4018356, https://doi.org/10.1061/(ASCE)MT.1943-5533.0002561.

Pougatchenkova, G.A. (1968) 'Les monuments peu connus de l'architecture médiévalede l'Afghanistan', *Afghanistan*, Vol. 21, No. 1, pp.17–27.

Rotunno, T., Rovero, L., Tonietti, U. and Bati, S.B. (2014) 'Experimental study of bond behavior of CFRP-to-Brick joints', *J. Compos. Constr.*, Vol. 19, p.4014063, https://doi.org/10.1061/(ASCE)CC.1943-5614.0000528.

Rovero, L. and Tonietti, U. (2012) 'Structural behaviour of earthen corbelled domes in the Aleppo's region', *Mater. Struct. Constr.*, Vol. 45, pp.171–184, https://doi.org/10.1617/S11527-011-9758-1/FIGURES/15.

Rovero, L., Galassi, S. and Misseri, G. (2020a) 'Experimental and analytical investigation of bond behavior in glass fiber-reinforced composites based on gypsum and cement matrices', *Compos. Part B Eng.*, Vol. 194, p.108051, https://doi.org/10.1016/j.compositesb.2020.108051.

Rovero, L., Galassi, S. and Misseri, G. (2020b) 'Experimental and analytical investigation of bond behavior in glass fiber-reinforced composites based on gypsum and cement matrices', *Compos. Part B Eng.*, Vol. 194, p.108051, https://doi.org/10.1016/j.compositesb.2020.108051.

Torrealva, D., Cerrón, C. and Espinoza, Y. (2008) 'Shear and out of plane bending strength of adobe walls externally reinforced with propylene grids', in *The 14th World Conference on Earthquake Engineering*, Beijin, China, pp.18–24.

Vegas, F., Mileto, C., Ivorra, S. and Baeza, F.J. (2012) 'Checking gypsum as structural material', *Appl. Mech. Mater.*, Vols. 117–119, pp.1576–1579, https://doi.org/10.4028/WWW.SCIENTIFIC.NET/AMM.117-119.1576.

Zampieri, P. (2020) 'Horizontal capacity of single-span masonry bridges with intrados FRCM strengthening', *Compos. Struct.*, Vol. 244, https://doi.org/10.1016/j.compstruct.2020.112238.

Zampieri, P., Simoncelo, N., Tetougueni, C.D. and Pellegrino, C. (2018) 'A review of methods for strengthening of masonry arches with composite materials', *Eng. Struct.*, Vol. 171, pp.154–169, https://doi.org/10.1016/J.ENGSTRUCT.2018.05.070.